Electrolyte Reactivity in the Double Layer in Mg Batteries: An Interface Potential-Dependent DFT Study

Anja Kopač Lautar, Jan Bitenc, Tomaž Rejec, Robert Dominko, Jean-Sébastien Filhol, Marie-Liesse Doublet

Electrolyte Reactivity in the Double Layer in Mg Batteries: An interface potential-dependent DFT Study

Anja Kopač Lautar[1, 2], Jan Bitenc[1], Tomaž Rejec[2, 3], Robert Dominko[1, 4, 5]
Jean-Sébastien Filhol[*, 6, 7] Marie-Liesse Doublet[6, 7]

[1]*Department of Materials Chemistry, National Institute of Chemistry, Slovenia*
[2]*Department of Physics, Faculty of Mathematics and Physics, University of Ljubljana, Slovenia*
[3]*Jozef Stefan Institute, Ljubljana, Slovenia*
[4]*Faculty of Chemistry and Chemical Technology, University of Ljubljana, Slovenia*
[5]*ALISTORE-ERI, FR3104, 80039 Amiens cedex, France*
[6]*ICGM, Univ Montpellier, CNRS, ENSCM, Montpellier, France*
[7]*RS2E French network on Electrochemical Energy Storage, FR5439, Amiens, France*
Corresponding author: Jean-Sébastien Filhol (jean-sebastien.filhol@umontpellier.fr)

Abstract

The electrochemical degradation of two solvent-based electrolytes for Mg-metal batteries is investigated through a Grand canonical DFT approach. Both electrolytes are highly reactive in the double layer region where the solvated species have no direct contact with the Mg-surface, hence emphasising that surface reactions are not the only phenomena responsible for electrolyte degradation. Applied to dimethoxyethane (DME) and ethylene carbonate (EC), the present methodology shows that both solvents should thermodynamically decompose in the double layer prior to the Mg^{2+}/Mg^{0} reduction, leading to electrochemically inactive reaction products. Based on thermodynamic considerations, Mg^{0} deposition should not be possible, which is not in agreement with experiments, at least for DME-based electrolytes. This apparent contradiction is here addressed through the rationalization of the electrochemical mechanism underlying solvent electro-activation. An extended *operation potential window* (OPW) is defined, in which the Mg^{2+}/Mg^{0} reduction can compete with electrolyte decomposition, thus enabling battery operation beyond the solvated species thermodynamic stability. The chemical study of the degradation products is in excellent agreement with experiments and it offer rationale for the Mg-battery failure in EC electrolyte and

capacity fade in DME electrolyte. Potential-dependent approach proposed herein is thus able to successfully tackle the challenging problem of interface electrochemistry. Being fully transferable to any other electrochemical systems, this methodology should provide rational guidelines for the development of viable electrolytes for multivalent batteries, and more generally, energy conversion and storage devices.

Introduction

Electrochemical interfaces play important roles in charge and mass transport in different electrochemical storage devices. Interactions between the composite electrode and the electrolyte are critical for long-term operation, and their understanding is crucial for the development of novel battery chemistries. The success of Li-ion battery technology is based on lithium conductive solid electrolyte interphases (SEI). However, full understanding of SEIs and their role on the battery performance is still under debate. This is partially due to the fact that microscopic phenomena occurring at the electrode/electrolyte interfaces are difficult to capture, both by experimental measurements and by conventional theoretical approaches.

Multivalent metal batteries are considered as alternative energy storage devices that can fulfil the demands of modern society for batteries. Among the different technologies, magnesium batteries have been investigated as safer and cheaper high-energy-density alternatives to Li-ion.[1–8] However, their development has been hindered by the lack of suitable hosting structures on the cathode side and limited availability of magnesium electrolytes.[9–12] A logical translation of existing electrolyte knowledge from lithium to magnesium batteries led to large overpotentials for stripping/deposition processes.[3,13,14]. That recoils a complete new type of electrolytes where combination of $Mg(TFSI)_2$ salt (TFSI=bis(trifluoromethane-sulfonyl)imidate) and dimetoxyethane (DME) as an ether solvent become particularly attractive due to improved electrochemical reversibility of Mg deposition, although it is still far from commercially accepted.[3,15,16] Note that $MgCl_2$ additives to DME-based electrolytes were also proven beneficial for cycling performance.[16–18]

While few experimental methods are able to probe interface processes,[2,3,10–12,19–21] theoretical approaches are even scarcer and mainly focus either on bulk electrodes or bulk electrolytes.[9,22–30] Previous theoretical works based on *ab initio* calculations and classical molecular dynamics simulations have provided useful

information on solvation structures,[9,22,24–26,28,29] ion pair formation,[9,22,29] dynamical properties,[24–26] and stability of the system.[9,10,22–25,27,28] Such studies are valuable for understanding bulk electrolyte thermodynamics and dynamics as a function of liquid components and concentrations. However, properties obtained for the bulk are not transferable to interfacial electrochemistry where the electrolyte properties are altered by strong electric fields that can reach over 10^9 V/m. This strongly alters the electron transfer through the electrical double layer,[31] which in turns affects the thermodynamics and kinetics of the electrochemical processes.[32,33] The impact of the electric field on the electrolyte reactivity may spread over a couple of nanometres from the surface. Hence, while decomposition of the adsorbed species at the Mg-metal anode is often regarded as the main origin of the formation of the passivation layer,[11,34,35] these chemically-driven reactions are presumably concomitant with other electrochemically activated reactions occurring in the double layer. Within the so-called outer Helmholtz plane of the electrochemical double layer, electron transfer or tunnelling may occur between the surface and the solvated species without direct adsorption on the surface. Therefore, electrochemical activation in the double layer may lead to a specific reactivity of the electrolyte that can be critical for the electrolyte stability as it induces either a beneficial SEI or a detrimental passivation films.

Up to now, the stability of electrolytes has generally been investigated through molecular *ab initio* calculations focussing on the energy difference between the highest occupied molecular orbital (HOMO) and the lowest unoccupied molecular orbital (LUMO) of the solvated species as the pertinent descriptor.[36,37] Such a zero-order approach neglects the electrochemical response of the system, i.e. the electrode/electrolyte electron transfer which is required to maintain the two components at the same electrochemical potential. To overcome this issue, an explicit interface comprising both the electrode and the electrolyte must be modelled as a function of the electrochemical potential. Indeed, interface reactivity strongly depends on the operating voltage and needs to be investigated through a potential-dependent *ab initio* approach. Theoretical works in this direction have been proposed in the field of electro-catalysis or corrosion, each of them relying on various approximations of the free electrochemical energy or the electrochemical double layer.[11,34–42] In the specific context of Li-ion batteries, an easy-handling and numerically affordable methodology was recently proposed to investigate the potential-dependent phenomena of such complex interfaces.[40] Previously validated on stable Li-metal/$Li(EC)_4^+$ [40] and Ru/H_2O interfaces,[43] the methodology is here extended to the

thermodynamic and electrochemical stability of Mg-metal/electrolyte interfaces on two different classes of solvents, namely ethylene-carbonate (EC) and dimethyl-ether (DME). This *ab initio* procedure allows determining the absolute Mg^{2+}/Mg^{0} redox potential in both solvents within an accuracy of few tens of millivolt, without any other parameter than the one defining the implicit solvent (see Computational Details in Supplementary Information,). Moreover, it enables to access the thermodynamic and electrochemical stability windows of the electrolytes which are further confirmed by experiments. A novel descriptor, namely the potential-dependent Fukui functions[39,44] is then introduced to unambiguously identify the redox centre of the electrochemical reactions as a function of the applied potential and the solvent. Finally, the methodology provides valuable information on solvent decomposition pathways and products, allowing full rationalization of the Mg-battery failure in EC-based electrolytes and capacity fading in DME-based electrolytes. We believe this methodology opens interesting prospects for a rational design of new electrolytes for multivalent batteries and, more generally, for meeting the current challenge of electrochemical interface in energy applications.

Results and discussion

The thermodynamic stability window of EC- and DME-based electrolytes were computed using the Grand canonical DFT approach reported previously[40,43,44] and described in Computational Details section of the SI. For both solvents, two interfaces corresponding to the reduced and oxidized members of the Mg^{2+}/Mg^{0} reaction were considered. The former consists of an Mg(0001)-surface immerged in a polarizable continuum medium (PCM)[45–47] to account for the electrolyte dielectric constant and properly describe the interface polarization, i.e. the surface capacitance of the electrode. One solvated Mg^{2+} species including its first solvation shell of solvents is then explicitly added to the reduced interface to describe the oxidized member of the reaction (**Fig. 1**). For both solvents, the solvated species were obtained from molecular first-principles calculations,[48] and correspond to $Mg(DME)_3^{2+}$ and $Mg(EC)_6^{2+}$ (SI and **Fig. S1**), in good agreement with previous works.[9,25,49]

For the interface electrochemical reactions (1-2), where Mg_s stands for the Mg-anode surface, the Mg^{2+}/Mg^{0} redox potential is predicted by our calculations to be –2.44 V and –2.39 V with respect to the standard hydrogen electrode (SHE) for $Mg(EC)_6^{2+}$ and $Mg(DME)_3^{2+}$, respectively (**Fig. 2a, A**).

$$[Mg_s\text{-}Mg(DME)_3^{2+}] + 2e^- \rightarrow Mg_s + Mg^0 + 3DME \quad (1)$$

$$[Mg_s\text{-}Mg(EC)_6^{2+}] + 2e^- \rightarrow Mg_s + Mg^0 + 6EC \quad (2)$$

These values are in excellent agreement with experimental data (–2.37 V_{SHE})[50] and assess the validity of the methodology in showing full consistency between computed energies and potentials.

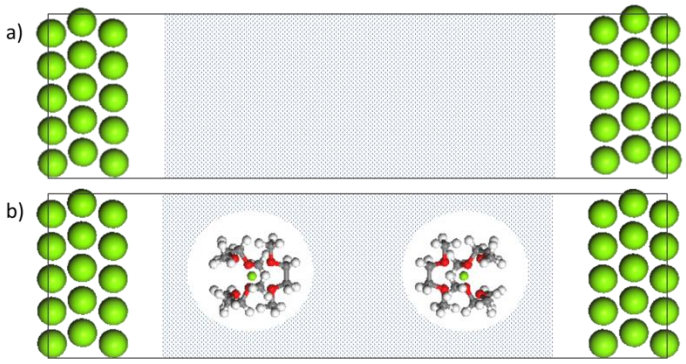

Figure 1: Description of the reduced and oxidized interface. (a) The reduced system consisting of Mg(0001)-surface and Mg^0. **(b)** The oxidized system takes into account the Mg(0001)-surface and solvated Mg complex, in this example $Mg(DME)_3^{2+}$. The polarization continuum media (PCM) is schematically depicted by the grey region. Mg, C, O and H atoms are respectively green, grey, red and white.

Both $Mg(EC)_6^{2+}$and $Mg(DME)_3^{2+}$ solvated species undergo a spontaneous transformation under extreme reductive conditions, i.e. at a potential below -3.2 V_{SHE} (**Fig. 2a, B**). This corresponds to a spinodal limit potential below which the oxidized interface no longer presents a local minimum in its potential-energy surface. According to our structural relaxations, $Mg(EC)_6^{2+}$ undergoes a dimerization of two EC molecules to form the neutral $Mg(EC)_4$(dimer) complex, while $Mg(DME)_3^{2+}$ dissociates into the neutral $Mg(OCH_3)_2(DME)_2$ complex and one ethylene molecule (C_2H_4) (**Fig. S2**). The free electrochemical energy of the as-formed products was then computed as a function of the potential, following the same procedure as for the initial reduced and oxidized interfaces (blue curves in **Fig. 2a**). Interestingly, these reduced interfaces become thermodynamically more stable than the initial Mg_s-$Mg(DME)_3^{2+}$ and Mg_s-$Mg(EC)_6^{2+}$ oxidized interfaces at potentials which are higher than the Mg^{2+}/Mg^0 reduction potential (**C vs. A in Fig. 2a**). The reduction of the initial solvated species is predicted to occur at –1.1 V_{SHE} for the DME and –1.6 V_{SHE} for EC, following reactions (3-4):

$$Mg_s\text{-}Mg(DME)_3^{2+} + 2e^- \rightarrow Mg_s\text{-}Mg^0(OCH_3)_2(DME)_2 + C_2H_4 \quad (3)$$

$$Mg_s\text{-}Mg(EC)_6^{2+} + 2e^- \rightarrow Mg_s\text{-}Mg^0(EC)_4(dimer) \quad (4)$$

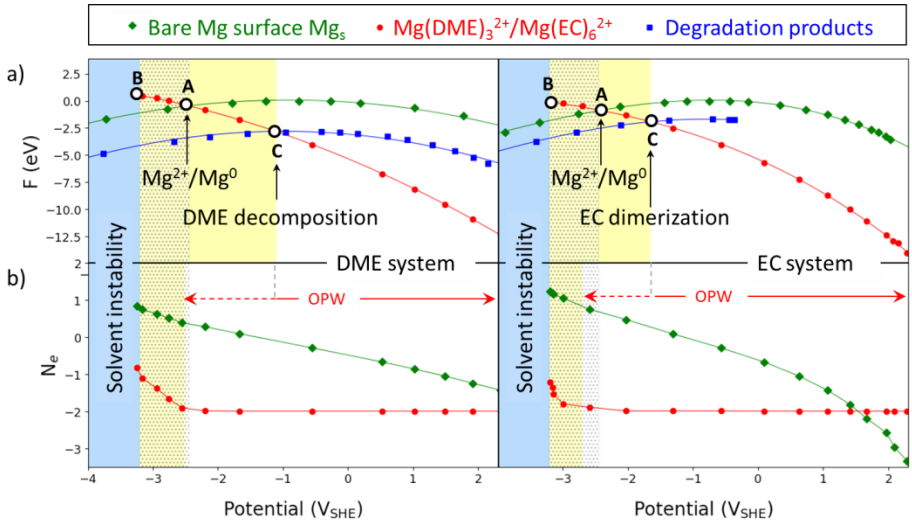

Figure 2. Potential-dependent thermodynamic stability of DME- and EC-based electrolytes **(a)** Free electrochemical energy (F) computed for the reduced (green) and oxidized (red) interfaces involved in the electrochemical reactions occurring at the electrode/electrolyte interfaces in DME-based (left) and EC-based (right) electrolytes. According to the present methodology, the potentials at which free electrochemical energies of the two interfaces cross corresponds to the equilibrium potential of the considered reaction. The letters mark potentials of importance: A) Equilibrium potential of the Mg^{2+}/Mg^0 redox pair; B) The initial oxidized interfaces including the Mg^{2+} solvated species in the electric double layer become unstable and undergo a spontaneous transformation into the decomposed (DME) or dimerized system (EC) (blue curves); C) Potential below which the solvent molecules in the solvation shell of the Mg^{2+} solvated species become thermodynamically unstable with respect to decomposition (DME-system) or dimerization (EC-system). **(b)** Net charge computed on the surface (green) and on the solvated species (red) as a function of the potential. The solvent only starts gaining electrons (i.e. starts to be metastable) at approximately –2.5 V_{SHE} and –2.7 V_{SHE} for the DME and EC system, respectively, which extends the operating potential window in comparison with the thermodynamic stable region (white region on Fig.2a vs Fig. 2b). Yellow zone gives solvent metastability potential domains, while the grey region indicates the start of the Mg^{2+} deposition to Mg surface.

Hence, while the unstable region of both DME and EC systems begins at approximately the same potential, $Mg(EC)_6^{2+}$ becomes metastable at a significantly lower potential than $Mg(DME)_3^{2+}$. Remarkably, these results indicate that the Mg^{2+}/Mg^0 reduction should be thermodynamically prevented in both electrolytes, as

the reduction of solvent in the first solvation shell occurs first at a higher potential. This is in apparent contradiction with experiments demonstrating an electrochemical cycling of Mg-metal batteries in DME-based electrolytes, although coming along with capacity fade.[15,16,51] In fact, the thermodynamic stability itself cannot be taken as the unique criterion for solvent stability/reactivity. Slow kinetics can widen the electrochemical stability window as is utilized in many applications, such as polarography or zinc electroplating in aqueous solvents. When the kinetic rate of solvent degradation is far slower than Mg-plating reaction, an extended potential window can be defined to explain why the battery can operate, at least in short-term cycling, beyond the strict thermodynamic limit. This extended potential window is here defined as the "operating potential window" (OPW) and is obtained by assuming that solvent decomposition only occurs through electrochemical activation, i.e. through electron transfer from or to the solvent molecule. This electron transfer can be easily evaluated from the net charge of the solvated species and is given in **Fig. 2b**. Clearly, it shows that the OPW is extended down to –2.5 V_{SHE} for DME and –2.7 V_{SHE} for EC. This is supported by a topological analysis of the electron density at both interfaces, through the computation of the potential-dependent Fukui functions. The Fukui function is a valuable tool to probe the highest occupied and lowest unoccupied states of an electronic structure[39] and is here used to identify the redox centre of an electrochemical reaction, at each given potential. Computed at –2.55 V_{SHE} for DME and –2.6 V_{SHE} for EC, the Fukui functions confirm the electrochemical activation of $Mg(DME)_3^{2+}$ and $Mg(EC)_6^{2+}$ through an electron transfer from the Mg-surface to the anti-bonding σ^* and π^* orbitals of DME and EC, respectively (**Figs. 3a and 4a**). This electrochemical activation is also supported by the projected density of states (PDOS). A shift of the Fermi level up to the LUMOs of $Mg(DME)_3^{2+}$ and $Mg(EC)_6^{2+}$ is clearly visible which induces an electron transfer from the Mg-surface to the solvated species (**Figs. 3b and 4b)**. There is no such electron transfer in the potential range where the solvent is electrochemically inactive, as the Fermi level lays in the HOMO/LUMO gap (**Figs. 3a and 4a**). Under oxidative conditions, there is electron transfer from solvated species to the Mg-surface (**Fig. S3**)

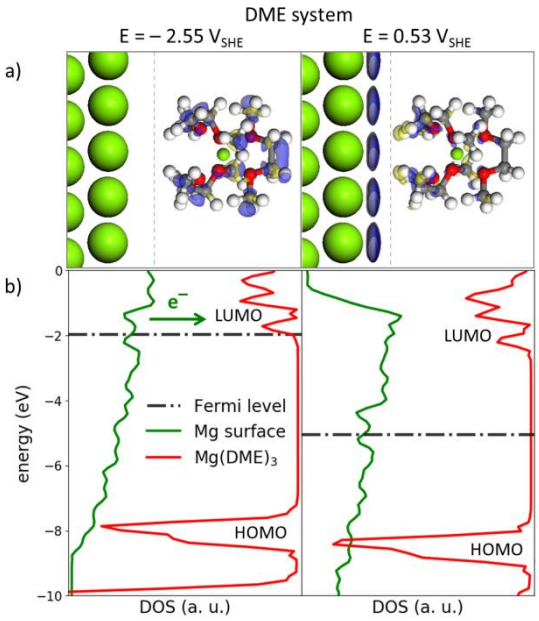

Figure 3. Chemical descriptors of the DME solvent reactivity. **(a)** Fukui functions computed for the Mg$_s$-Mg(DME)$_3^{2+}$ oxidized interface at reductive potential (–2.55 V$_{SHE}$) and in the inactive region (0.53 V$_{SHE}$). The positive contribution of the Fukui function (blue volumes) allows identifying the redox centre of the electrochemical reaction (reduction or oxidation). Fukui function at the reductive potential shows that the electrochemical activation of Mg(DME)$_3^{2+}$ occurs through an electron transfer from the Mg-surface to the anti-bonding σ^* orbitals of DME. In the inactive region only the Mg-surface is activated, while the Mg(DME)$_3^{2+}$ only shows polarization effect (same amount of positive and negative (blue and yellow, respectively) contributions of the Fukui function). Note that the empty space between the surface and the solvated species was decreased for clarity sake. **(b)** PDOS were computed for the surface and Mg(DME)$_3^{2+}$ at the same potential as the Fukui functions. At the reductive potential the Fermi level reaches the LUMO of the Mg(DME)$_3^{2+}$ and electron transfer from Mg-surface to the Mg(DME)$_3^{2+}$ is induced. In inactive region, the Fermi level is in the HOMO/LUMO gap, making electron transfer impossible. All energies are referenced relatively to the vacuum level.

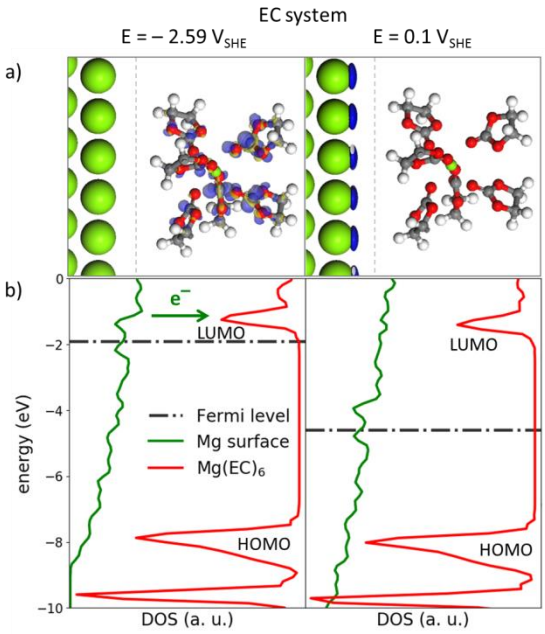

Figure 4. Chemical descriptors of the EC solvent reactivity. **(a)** Fukui functions computed for the Mg_s-$Mg(EC)_6^{2+}$ oxidized interface at reductive potential (–2.59 V_{SHE}) and in the inactive region (0.1 V_{SHE}). The positive contribution of the Fukui function (blue volumes) allows identifying the redox centre of the electrochemical reaction (reduction or oxidation). Fukui function at the reductive potential shows that the electrochemical activation of $Mg(EC)_6^{2+}$ occurs through an electron transfer from the Mg-surface to the anti-bonding π^* orbitals of EC. In the inactive region only the Mg-surface is electrochemically active, while the $Mg(EC)_6^{2+}$ only shows polarization effect (same amount of positive and negative (blue and yellow, respectively) contributions of the Fukui function). Note that the empty space between the surface and the solvated species was decreased for clarity sake. **(b)** PDOS were computed for the surface and on $Mg(EC)_6^{2+}$ at the same potentials as the Fukui functions. At the reductive potential the Fermi level reaches the LUMO of the $Mg(EC)_6^{2+}$ and electron transfer from Mg-surface to the $Mg(EC)_6^{2+}$ is induced. In inactive region, the Fermi level is in the HOMO/LUMO gap, making electron transfer impossible. All energies are referenced relatively to the vacuum level.

Overall, these results demonstrate that solvent decomposition in the first solvation shell of Mg^{2+} can occur in the double layer of the Mg-electrode/electrolyte interfaces and that surface reactions are not the only origin of electrolyte degradation. A competitive reduction mechanism between the Mg^{2+} cation and the organic solvents is also shown to exist in EC-based and DME-based electrolytes which might turn to Mg-deposition, owing to the low kinetic rates of solvent decomposition. Noteworthy, the investigation of the electrochemical stability/reactivity of free EC and DME solvents (not coordinated to Mg^{2+}) using the same methodology reveals that both solvents show high electrochemical

stability down to very low potentials (–4 V_{SHE}) in agreement with their LUMO remaining far above the Mg^{2+}/Mg^0 redox energy (**Figs. S4, S5, and S6**). Free EC is shown to be kinetically stable (no electron transfer) in oxidative conditions, as well, up to 2-2.5 V_{SHE} which justifies the wide use of alkyl carbonates in the battery technology (**Fig. S4 and S6**). In contrast, free DME is sensitive to oxidation above 1 V_{SHE} due to the activation of its oxygen lone-pairs (**Fig. S4 and S5**) hence leading to a possible DME oxidation / peroxidation at higher potentials.[52–54]

The remaining question is to figure out the origin of the different electrochemical performance experimentally observed for Mg-metal batteries cycled in EC- or DME-based electrolytes. While both solvent-based electrolytes display wide enough OPW to enable Mg^{2+}/Mg^0 reduction, experimental facts show a battery failure in EC and a reasonable, yet short-term cycling in DME. Although very instructive, the comparison between the thermodynamic and electro-kinetic stability windows of $Mg(DME)_3^{2+}$ and $Mg(EC)_6^{2+}$ does not provide definite conclusion on the suitability of a solvent to be used in Mg-metal battery electrolytes. To address this point, it is necessary to figure out the impact of each solvent degradation products on the overall performance of the electrolytes. In particular, the substantial differences found in the reduction mechanism of DME and EC need to be thoroughly examined. In the case of EC, the formation of $Mg(EC)_4$(dimer) results from the reduction of the C=O double bond of two over six EC molecules formally into $\bullet C–O^-$. Consequently, a spontaneous EC dimerization through the formation of one C–C bond between two adjacent carbonate groups occurs, leading to a neutral *orthoester*-like complex. Such transformation could have been anticipated from the potential-dependent Fukui function computed at –2.6 V_{SHE} which clearly shows the activation of the anti-bonding π^* orbitals of two EC molecules (**Fig. 4a**). Furthermore, structural relaxations show a significant increase of the C–O bond-length in the dimer ring from 1.35 Å to 1.51 Å. These results suggest that the EC-dimer is activated and prone to ring opening, which in turn initiates chain polymerization of free EC molecules.[55] Consequently, a significant fraction of solvent around the Mg-electrode surface should rapidly convert into a compact polymer, and form a passive layer over the electrode surface. This suddenly prevents ionic diffusion through the interface and sharply increases the negative electrode impedance.[3,13,14,56] Such a mechanism is clearly consistent with previous reports on Mg-metal batteries cycled in EC-based electrolytes.[14,55] Noteworthy, our previous investigation of $Li_s/Li(EC)_4^+$ interface reactivity has not shown any spontaneous dimerization of EC down to highly reducing potential (–3.8 V_{SHE}). This can be attributed to the lower electrophilic character of Li^+ compared to Mg^{2+}, which

prevents easy solvent reactivity, although EC molecules are still found to be activated by electronic transfer.[40] In Li-ion batteries, the better performance of EC-based electrolytes possibly arise either from a less efficient polymerisation of the EC solvents due to a lower coordination number in the cation solvation shell (4 for Li^+ and 6 for Mg^{2+}), charge effect or from an easier Li^+ diffusion through the passive layer.

In the case of DME, the decomposition under highly reductive potentials arises from the C–O bond breaking of one over three molecules. Once again, this is fully predicted by the potential-dependent Fukui function showing the activation of the anti-bonding σ^* orbitals of the external DME (**Fig. 3a**). The product of decomposition, namely ethylene, was already observed in in Li-ion batteries using electrolytes with DME as a solvent.[57] Interestingly, the DME fragmentation enables significant reorganization of the electron density of the complex, through the shortening of the Mg–OCH_3 bonds from 2.12 Å to 1.91 Å and the concomitant elongation of the Mg–O_{DME} bonds from 2.12 Å to 2.3 Å, which significantly decreases the Mg electrophilicity. As the $Mg(OCH_3)_2(DME)_2$ products is stable under further reduction, its formation should prevent further reduction of the remaining solvents in the Mg^{2+} solvation shell but also of Mg^{2+} into Mg^0. This is corroborated by our calculations which predict that the complete reduction of the $Mg(OCH_3)_2(DME)_2$ complex into Mg^0 only occurs at –3.9 V_{SHE} (**Figs. S7 and S8**). Such a low potential is consistent with the necessary formation of a hard Pearson base (i.e. CH_3O^-) that is poorly solvated by ethereal solvent, in sharp contrast to soft bases such as $TFSI^-$.[58] The precipitation of the electro-inactive $Mg(OCH_3)_2(DME)_2$ should thus progressively degrade the electrolyte through the loss of active Mg^{2+} leading to battery capacity fade on cycling.

In order to validate our theoretical predictions, cyclic voltammetry measurements were carried out on a Pt working electrode in the EC and DME solvents with 0.4M $Mg(TFSI)_2$. Results confirm the better performance of the DME system compared to the EC system (**Fig. 5**). In EC-based electrolytes, the first electrochemical cycle reveals a reduction peak at –2.9 V_{SHE} and a small oxidation peak at –1.4 V_{SHE}. The intensity of both peaks significantly decreases in further cycles, leading rapidly to a plain capacitive response after a few cycles (i.e. electrode failure). This clearly points to passivation of the Pt working electrode in this solvent, in agreement with our theoretical assumption that $Mg(EC)_4$(dimer) products initiate EC polymerization, hence leading to the formation of an insulating layer at the surface of the electrode. The

reduction/oxidation peak at –1.4 V_{SHE} is presumably connected with partial reversibility of the EC solvent dimerization, which is computationally predicted at a reasonably close potential (–1.6 V_{SHE} at thermodynamic equilibrium). Measurements in the DME solvent exhibit a well-defined Mg deposition peak (reduction) starting at –3.1 V_{SHE}, associated with a current-intensity 50 times higher than in EC solvent. The Mg-metal stripping peak (oxidation) is positioned at a significantly higher potential of –0.4 V_{SHE}, which points to some quasi-passivation of the Mg-metal deposited on the Pt electrode. The coulombic efficiency is quite low at around 30%, which could be attributed to side reactions (e.g. solvent reduction) during the Mg deposition and/or loss of deposited Mg due to passivation by electrolyte species. Upon further cycles, both deposition and stripping peaks can be identified, which clearly indicates that partial cycling is achieved in DME solvents. However, the intensity of the stripping peak decreases and the peak broadens. This could point to both increased contribution from side reactions during Mg deposition in later cycles and gradual accumulation of Mg passivating species on the working electrode with continued cycling (**Fig. 5**).

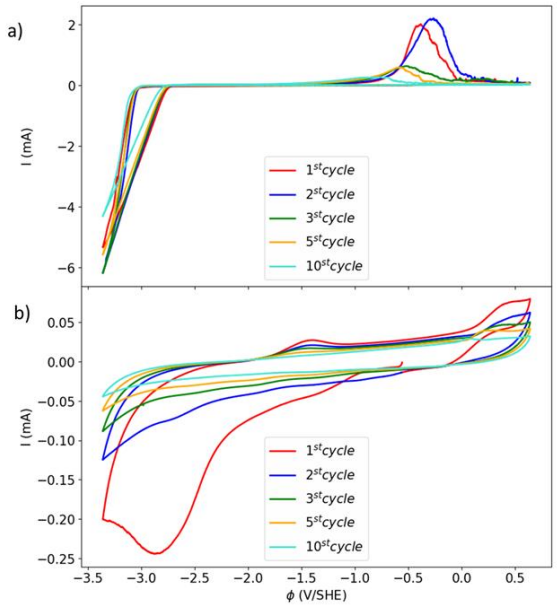

Figure 5. Experimental confirmation of theoretical predictions. (a) Cyclic voltammetry on Pt working electrode in 0.4M $Mg(TFSI)_2$ in DME. Sweep rate 25 mV/s, with Mg metal as counter electrode and Printex carbon reference electrode. **(b)** Cyclic voltammetry on Pt working electrode in 0.4M $Mg(TFSI)_2$ in EC. Sweep rate 25 mV/s, with Mg metal as counter electrode and Printex carbon reference electrode.

Overall, these results clarify the origin of the inefficient Mg^{2+}/Mg^0 reduction in DME-based electrolytes, and makes it possible to understand the beneficial impact of chlorides in the Mg^{2+} solvation sphere, as reported in the literature.[17,18,59,60] The competition between DME and Mg^{2+} reduction leads to the formation of reduced $Mg(OCH_3)_2(DME)_2$ species. In this species, the magnesium can no longer be reduced at a reasonable potential and plated on the Mg electrode, as this would lead to the formation of hard CH_3O^- bases that are not stable in DME solvents. As a consequence, electrons are consumed by the reduction of DME, and Mg^{2+} ions are trapped in the $Mg(OCH_3)_2(DME)_2$ products. To prevent solvent reduction and improve electrolyte stability, the Mg^{2+} electrophilic activation must be reduced by the introduction of electron-donor species in its first solvation shell. This is exactly what is done when using mixtures of $Mg(TFSI)_2$ and $MgCl_2$ salts.[17,59] These mixtures lead to chlorinated complexes such as $Mg_2Cl_2(DME)_4$[18,61] in which the strongly polarized Mg–Cl bonds decrease the Mg^{2+} electrophilic activation of DME. Thus, the inclusion of the $MgCl_2$ salt prevents degradation, alike the electron-donor CH_3O^- ligands in the $Mg(OCH_3)_2(DME)_2$ products prevent further DME decomposition. While the reduction of $Mg(OCH_3)_2(DME)_2$ in Mg^0 was shown to occur at very low potentials, the substitution of OCH_3^- for Cl^- should allow Mg^{2+} reduction while still offering beneficial stabilization of the ancillary ligands. This rationale will be investigated in a forthcoming study. Eventually, another route for preventing undesired side-reactions could be to mix ethereal and carbonated solvents in order to control cyclic-carbonate polymerization and create a porous rather than dense SEI. This SEI would still allow Mg^{2+} diffusion while preventing solvated Mg^{2+} complex to enter the double layer region.

Conclusion

A Grand canonical DFT approach to electrochemical interfaces is used herein to capture the microscopic mechanisms of solvent degradation at the electrode/electrolyte interface in Mg-metal batteries. The potential-dependent reactivity of two classes of solvents, namely ethylene-carbonate (EC) and dimethyl-ether (DME) is elucidated with the help of accurate free electrochemical energy calculations and chemical bond analyses. Under reducing conditions, these solvents display different reaction pathways and degradation products that are both shown to be detrimental to the coulombic efficiency, and directly linked to the nature of the solvent O-R bonds (σ– or π–type). In the case of EC solvent, the reduction of $Mg(EC)_6^{2+}$

into a neutral $Mg(EC)_4$(dimer) complex in the outer Helmholtz plane leads to chain polymerisation, ending with the formation of a passive layer at the Mg-electrode surface that prevents Mg^0 deposition. In the case of DME, the competition between DME and Mg^{2+} reduction leads to the formation of an inactive $Mg(OCH_3)_2(DME)_2$ species that progressively coats the electrode surface hindering cycling. Cyclic voltammetry measurements carried out on a Pt working electrodes in EC- and DME-based electrolytes reveal electrochemical behaviours in fair coherence with these theoretical predictions. This opens interesting prospects for the present methodology to be used as a valuable characterization tool to assess the suitability of other solvent-based electrolytes. Among the various prospects of this work, the role of magnesium salts on the overall stability/reactivity of Mg-battery electrolytes, as well as the dynamics of Mg^{2+} diffusion at the interface (with and without SEI) are of primary importance. Remarkably, the present study already suggests that electron-donor anions included in the Mg^{2+} solvation shell should act as a stabilizer for DME decomposition in the double layer, as evidenced with chlorides. Eventually, the present methodology is easy transferable to any type of electrochemical reactions, therefore opening new prospects for investigating interfaces in wide application domains from corrosion to energy storage and conversion.

Supporting Information

- S1. Computational details.
- S2. Experimental details.
- Figure S1. Determination of the first solvation shell of Mg^{2+} in DME and EC solvent.
- Figure S2. Spontaneous reduction of Mg^{2+} solvation shell.
- Figure S3. Chemical descriptors of the DME and EC solvent reactivity.
- Figure S4. Potential-dependent thermodynamic stability of DME- and EC-based electrolytes and free DME and EC solvent molecules.
- Figure S5. Chemical descriptors of the free DME solvent molecule reactivity.
- Figure S6. Chemical descriptors of the free EC solvent molecule reactivity.
- Figure S7. Potential dependence of free electrochemical energy for different system in monoglyme solvent.
- Figure S8. Models for calculating the reduction potential of decomposed Mg^{2+} solvation shell in DME.
- Figure S9. Cyclic voltammetry on Pt working electrode.
- cif files of the different interfaces obtained with $Mg(DME)_3^{2+}$, $Mg(OCH_3)_2(DME)_2$, $Mg(EC)_6^{2+}$ and $Mg(EC)_4$(dimer)

Acknowledgements

MLD and JSF thank the French National Research Agency for its support through the Labex STORE-EX project (ANR-10LABX-76-01). Part of this work was supported by EU through the POROUS4APP project (H2020-NMP-PILOTS-2015n n°686163). Financial support from the Slovenian Research Agency (research project J2-8167, research core funding P2-0393 and P1-0044) and Honda R&D Europe (Germany) is gratefully acknowledged and appreciated. MLD, RD and AKL also acknowledge the PROTEUS PHP

program of Campus France for supporting AKL travelling expenses through the MAGINTER project (N° 40097SG). This work was performed using HPC resources from GENCI-CINES (Grant 2019-A0060910369).

References

(1) Aurbach, D.; Gofer, Y.; Schechter, A.; Chusid, O.; Gizbar, H.; Cohen, Y.; Moshkovich, M.; Turgeman, R. A Comparison between the Electrochemical Behavior of Reversible Magnesium and Lithium Electrodes. *J. Power Sources* **2001**, *97–98*, 269–273. https://doi.org/10.1016/S0378-7753(01)00622-X.

(2) Mohtadi, R.; Mizuno, F. Magnesium Batteries: Current State of the Art, Issues and Future Perspectives. *Beilstein J. Nanotechnol.* **2014**, *5*, 1291–1311. https://doi.org/10.3762/bjnano.5.143.

(3) Erickson, E. M.; Markevich, E.; Salitra, G.; Sharon, D.; Hirshberg, D.; de la Llave, E.; Shterenberg, I.; Rozenman, A.; Frimer, A.; Aurbach, D. Review—Development of Advanced Rechargeable Batteries: A Continuous Challenge in the Choice of Suitable Electrolyte Solutions. *J. Electrochem. Soc.* **2015**, *162* (14), 2424–2438. https://doi.org/10.1149/2.0051514jes.

(4) Matsui, M. Study on Electrochemically Deposited Mg Metal. *J. Power Sources* **2011**, *196*, 7048–7055. https://doi.org/10.1016/j.jpowsour.2010.11.141.

(5) Jäckle, M.; Groß, A. Microscopic Properties of Lithium , Sodium , and Magnesium Battery Anode Materials Related to Possible Dendrite Growth Related to Possible Dendrite Growth. *J. Chem. Phys.* **2014**, *141*, 174710. https://doi.org/10.1063/1.4901055.

(6) Ling, C.; Banerjee, D.; Matsui, M. Study of the Electrochemical Deposition of Mg in the Atomic Level: Why It Prefers the Non-Dendritic Morphology. *Electrochim. Acta* **2012**, *76*, 270–274. https://doi.org/10.1016/j.electacta.2012.05.001.

(7) Jäckle, M.; Helmbrecht, K.; Smits, M.; Stottmeister, D.; Groß, A. Self-Diffusion Barriers : Possible Descriptors for Dendrite Growth in Batteries? *Energy Environ. Sci.* **2018**, *11*, 3400–3407. https://doi.org/10.1039/c8ee01448e.

(8) Kopač Lautar, A.; Kopač, D.; Rejec, T.; Bančič, T.; Dominko, R. Morphology Evolution of Magnesium Facets : DFT and KMC Simulations. *Phys. Chem. Chem. Phys.* **2019**, *21*, 2434–2442. https://doi.org/10.1039/c8cp06171h.

(9) Rajput, N. N.; Qu, X.; Sa, N.; Burrell, A. K.; Persson, K. A. The Coupling between Stability and Ion Pair Formation in Magnesium Electrolytes from First-Principles Quantum Mechanics and Classical Molecular Dynamics. *J. Am. Chem. Soc.* **2015**. https://doi.org/10.1021/jacs.5b01004.

(10) Dong, S.; Kim, Y.; Lee, S.-S.; Kim, D. Y.; Lim, Y.; Roy, B.; Ryu, Y.-G. Operating Mechanisms of Electrolytes in Magnesium Ion Batteries: Chemical Equilibrium, Magnesium Deposition, and Electrolyte Oxidation. *Phys. Chem. Chem. Phys.* **2014**, *16* (16), 25789–25798. https://doi.org/10.1039/c4cp01259c.

(11) Yu, Y.; Baskin, A.; Valero-Vidal, C.; Hahn, N. T.; Liu, Q.; Zavadil, K. R.; Eichhorn, B. W.; Prendergast, D.; Crumlin, E. J. Instability at the Electrode/Electrolyte Interface Induced by Hard Cation Chelation and Nucleophilic Attack. *Chem. Mater.* **2017**, *29* (19), 8504–8512. https://doi.org/10.1021/acs.chemmater.7b03404.

(12) Tutusaus, O.; Mohtadi, R.; Singh, N.; Arthur, T. S.; Mizuno, F. Study of Electrochemical Phenomena Observed at the Mg Metal/Electrolyte Interface. *ACS Energy Lett.* **2016**, *2*, 224–229. https://doi.org/10.1021/acsenergylett.6b00549.

(13) Lu, Z.; Schechter, A.; Moshkovich, M.; Aurbach, D. On the Electrochemical Behavior of Magnesium Electrodes in Polar Aprotic Electrolyte Solutions. *J. Electroanal. Chem.* **1999**, *466*, 203–217. https://doi.org/10.1016/S0022-0728(99)00146-1.

(14) Bucur, C. B.; Gregory, T. D. *Challenges of a Rechargeable Magnesium Battery*, 2nd Editio.; Springer, 2018.

(15) Ha, S.-Y.; Lee, Y.-W.; Koo, B.; Kim, J.-S.; Cho, J.; Lee, K. T.; Choi, N.-S. Magnesium(II) Bis(Trifluoromethane Sulfonyl) Imide-Based Electrolytes with Wide Electrochemical Windows for Rechargeable Magnesium Batteries. *ACS Appl. Mater. Interfaces* **2014**, *6* (6), 4063–4093. https://doi.org/10.1021/am405619v.

(16) Shterenberg, I.; Salama, M.; Yoo, H. D.; Gofer, Y.; Park, J.-B.; Sun, Y.-K.; Aurbach, D. Evaluation of $(CF_3SO_2)_2N^-$ (TFSI) Based Electrolyte Solutions for Mg Batteries. *J. Electrochem. Soc.* **2015**, *162* (13), 7118–7128. https://doi.org/10.1149/2.0161513jes.

(17) Bitenc, J.; Firm, M.; Randon Vitanova, A.; Dominko, R. Effect of Cl^- and $TFSI^-$ Anions on Dual Electrolyte Systems in a Hybrid $Mg/Li_4Ti_5O_{12}$ Battery. *Electrochem. commun.* **2017**, *76*, 29–33. https://doi.org/10.1016/j.elecom.2017.01.013.

(18) Barile, C. J.; Nuzzo, R. G.; Gewirth, A. A. Exploring Salt and Solvent Effects in Chloride-Based Electrolytes for Magnesium Electrodeposition and Dissolution. *J. Phys. Chem. C* **2015**. https://doi.org/10.1021/acs.jpcc.5b03508.
(19) Nellist, M. R.; Laskowski, F. A. L.; Qiu, J.; Hajibabaei, H.; Sivula, K.; Hamann, T. W.; Boettcher, S. W. Potential-Sensing Electrochemical Atomic Force Microscopy for in Operando Analysis of Water-Splitting Catalysts and Interfaces. *Nat. Energy* **2018**, *3*, 46. https://doi.org/10.1038/s41560-017-0048-1.
(20) Drvarič Talian, S.; Moškon, J.; Dominko, R.; Gaberšček, M. Reactivity and Diffusivity of Li Polysulfides: A Fundamental Study Using Impedance Spectroscopy. *ACS Appl. Mater. Interfaces* **2017**, *9* (35), 29760–29770. https://doi.org/10.1021/acsami.7b08317.
(21) Baloch, M.; Vizintin, A.; Chellappan, R. K.; Moskon, J.; Shanmukaraj, D.; Dedryvère, R.; Rojo, T.; Dominko, R. Application of Gel Polymer Electrolytes Based on Ionic Liquids in Lithium-Sulfur Batteries. *J. Electrochem. Soc.* **2016**, *163* (10), A2390–A2398. https://doi.org/10.1149/2.1151610jes.
(22) Lapidus, S. H.; Rajput, N. N.; Qu, X.; Chapman, K. W.; Persson, K. A.; Chupas, P. J. Solvation Structure and Energetics of Electrolytes for Multivalent Energy Storage. *Phys. Chem. Chem. Phys.* **2014**, *16* (40), 21941–21945. https://doi.org/10.1039/c4cp03015j.
(23) Ong, S. P.; Andreussi, O.; Wu, Y.; Marzari, N.; Ceder, G. Electrochemical Windows of Room-Temperature Ionic Liquids from Molecular Dynamics and Density Functional Theory Calculations. *Chem. Mater.* **2011**, *23* (11), 2979–2986. https://doi.org/10.1021/cm200679y.
(24) Hu, J. Z.; Rajput, N. N.; Wan, C.; Shao, Y.; Deng, X.; Jaegers, N. R.; Hu, M.; Chen, Y.; Shin, Y.; Monk, J.; et al. 25Mg NMR and Computational Modeling Studies of the Solvation Structures and Molecular Dynamics in Magnesium Based Liquid Electrolytes. *Nano Energy* **2018**, *46*, 436–446. https://doi.org/10.1016/j.nanoen.2018.01.051.
(25) Kubisiak, P.; Eilmes, A. Solvation of Mg^{2+} Ion in $Mg(TFSI)_2$/Dimethoxyethane Electrolytes - A View from Molecular Dynamics Simulations. *J. Phys. Chem. C* **2018**, *122* (24), 12615–12622. https://doi.org/10.1021/acs.jpcc.8b02460.
(26) Sa, N.; Rajput, N. N.; Wang, H.; Key, B.; Ferrandon, M.; Srinivasan, V.; Persson, K. A.; Burrell, A. K.; Vaughey, J. T. Concentration Dependent Electrochemical Properties and Structural Analysis of a Simple Magnesium Electrolyte: Magnesium Bis(Trifluoromethane Sulfonyl)Imide in Diglyme. *RSC Adv.* **2016**, *6* (114), 113663–113670. https://doi.org/10.1039/c6ra22816j.
(27) Jónsson, E.; Johansson, P. Electrochemical Oxidation Stability of Anions for Modern Battery Electrolytes: A CBS and DFT Study. *Phys. Chem. Chem. Phys.* **2015**, *17* (5), 3697–3703. https://doi.org/10.1039/C4CP04592K.
(28) Pour, N.; Gofer, Y.; Major, D. T.; Aurbach, D. Structural Analysis of Electrolyte Solutions for Rechargeable Mg Batteries by Stereoscopic Means and DFT Calculations. *J. Am. Chem. Soc.* **2011**. https://doi.org/10.1021/ja1098512.
(29) Callahan, K. M.; Casillas-Ituarte, N. N.; Roeselová, M.; Allen, H. C.; Tobias, D. J. Solvation of Magnesium Dication: Molecular Dynamics Simulation and Vibrational Spectroscopic Study of Magnesium Chloride in Aqueous Solutions. *J. Phys. Chem. A* **2010**, *114* (15), 5141–5148. https://doi.org/10.1021/jp909132a.
(30) Wang, Y.; Nakamura, S.; Makoto Ue, A.; Balbuena, P. B. Theoretical Studies To Understand Surface Chemistry on Carbon Anodes for Lithium-Ion Batteries: Reduction Mechanisms of Ethylene Carbonate. *J. Am. Chem. Soc.* **2001**, *123*, 11708–11718. https://doi.org/10.1021/JA0164529.
(31) Schmickler, W.; Santos, E. *Interfacial Electrochemistry*, 2nd Editio.; Springer, 2010.
(32) Bard, A. J.; Abruña, H. D.; Chidsey, C. E.; Faulkner, L. R.; Feldberg, S. W.; Itaya, K.; Majda, M.; Melroy, O.; Murray, R. W.; Porter, M. D.; et al. The Electrode/Electrolyte Interface - A Status Report. *J. Phys. Chem.* **1993**, *97* (28), 7147–7173. https://doi.org/10.1021/j100130a007.
(33) Bard, A. J.; Faulkner, L. R. *Electrochemical Methods*; 2001.
(34) Lowe, J. S.; Siegel, D. J. Reaction Pathways for Solvent Decomposition on Magnesium Anodes. *J. Phys. Chem. C* **2018**, *122* (20), 10714–10724. https://doi.org/10.1021/acs.jpcc.8b01752.
(35) Canepa, P.; Gautam, G. S.; Malik, R.; Jayaraman, S.; Rong, Z.; Zavadil, K. R.; Persson, K.; Ceder, G. Understanding the Initial Stages of Reversible Mg Deposition and Stripping in Inorganic Nonaqueous Electrolytes. *Chem. Mater.* **2015**, *27* (9), 3317–3325. https://doi.org/10.1021/acs.chemmater.5b00389.
(36) Baskin, A.; Prendergast, D. Exploration of the Detailed Conditions for Reductive Stability of $Mg(TFSI)_2$ in Diglyme: Implications for Multivalent Electrolytes. *J. Phys. Chem. C* **2016**, *120* (7), 3583–3594.
(37) Kumar, N.; Siegel, D. J. Interface-Induced Renormalization of Electrolyte Energy Levels in Magnesium Batteries. *J. Phys. Chem. Lett.* **2016**. https://doi.org/10.1021/acs.jpclett.6b00091.
(38) Ando, Y.; Kawamura, Y.; Ikeshoji, T.; Otani, M. Electrochemical Reduction of an Anion for Ionic-Liquid

Molecules on a Lithium Electrode Studied by First-Principles Calculations. *Chem. Phys. Lett.* **2014**, *612*, 240–244. https://doi.org/10.1016/j.cplett.2014.08.028.
(39) Filhol, J. S.; Doublet, M. L. Conceptual Surface Electrochemistry and New Redox Descriptors. *J. Phys. Chem. C* **2014**, *118*, 19023–19031. https://doi.org/10.1021/jp502296p.
(40) Lespes, N.; Filhol, J. S. Using Implicit Solvent in Ab Initio Electrochemical Modeling: Investigating Li^+/Li Electrochemistry at a Li/Solvent Interface. *J. Chem. Theory Comput.* **2015**, *11* (7), 3375–3382. https://doi.org/10.1021/acs.jctc.5b00170.
(41) Nørskov, J. K.; Rossmeisl, J.; Logadottir, A.; Lindqvist, L.; Lyngby, D.; Jo, H. Origin of the Overpotential for Oxygen Reduction at a Fuel-Cell Cathode. *J. Phys. Chem. B* **2004**, *108*, 17886–17892. https://doi.org/10.1021/jp047349j.
(42) Dalverny, A. L.; Filhol, J. S.; Doublet, M. L. Interface Electrochemistry in Conversion Materials for Li-Ion Batteries. *J. Mater. Chem.* **2011**, *21* (27), 10134–10142. https://doi.org/10.1039/c0jm04202a.
(43) Lespes, N.; Filhol, J.-S. Using the Electrochemical Dimension to Build Water/Ru(0001) Phase Diagram. *Surf. Sci.* **2015**, *631*, 8–16. https://doi.org/10.1016/J.SUSC.2014.06.017.
(44) Mamatkulov, M.; Filhol, J. S. An Ab Initio Study of Electrochemical vs. Electromechanical Properties: The Case of CO Adsorbed on a Pt(111) Surface. *Phys. Chem. Chem. Phys.* **2011**, *13* (17), 7675–7684. https://doi.org/10.1039/c0cp01444c.
(45) Kresse, G.; Furthmüller, J. Efficiency of Ab-Initio Total Energy Calculations for Metals and Semiconductors Using a Plane-Wave Basis Set. *Comput. Mater. Sci.* **1996**, *6* (1), 15–50. https://doi.org/10.1016/0927-0256(96)00008-0.
(46) Kresse, G.; Furthmüller, J. Efficient Iterative Schemes for Ab Initio Total-Energy Calculations Using a Plane-Wave Basis Set. *Phys. Rev. B - Condens. Matter Mater. Phys.* **1996**, *54* (16), 11169–11186. https://doi.org/10.1103/PhysRevB.54.11169.
(47) Mathew, K.; Sundararaman, R.; Letchowrth-Weaver, K.; Arias, T. A.; Henning, R. G. Implicit Solvation Model for Density-Functional Study of Nanocrystal Surfaces and Reaction Pathways. *J. Chem. Phys.* **2014**, *8*, 084106.
(48) Frisch, M. J.; Trucks, G.; Schlegel, H.; Scuseria, G.; Robb, M.; Cheeseman, J.; Montgomery, J.; Vreven, T.; Kudin, K.; Burant, J.; et al. Gaussian 03, Revision C.02. **2004**.
(49) Salama, M.; Shterenberg, I.; Gizbar, H.; Eliaz, N. N.; Kosa, M.; Keinan-Adamsky, K.; Afri, M.; Shimon, L. J. W.; Gottlieb, H. E.; Major, D. T.; et al. Unique Behavior of Dimethoxyethane (DME)/$Mg(N(SO_2CF_3)_2)_2$Solutions. *J. Phys. Chem. C* **2016**, *120* (35), 19586–19594.
(50) Standard Reduction Potentials http://www5.csudh.edu/oliver/chemdata/data-e.htm (accessed Jun 13, 2019).
(51) Bitenc, J.; Pirnat, K.; Žagar, E.; Randon-Vitanova, A.; Dominko, R. Effect of Salts on the Electrochemical Performance of Mg Metal–organic Battery. *J. Power Sources* **2019**, *430* (April), 90–94. https://doi.org/10.1016/j.jpowsour.2019.04.114.
(52) Tamura, T.; Nakamura, M. Physicochemical Properties of Glyme - Li Salt Complexes as a New Family of Room-Temperature Ionic Liquids. *Chem. Lett.* **2010**, *39*, 753–755. https://doi.org/10.1246/cl.2010.753.
(53) Tobishima, S.; Morimoto, H.; Aoki, M.; Saito, Y.; Inose, T.; Fukumoto, T.; Kuryu, T. Glyme-Based Nonaqueous Electrolytes for Rechargeable Lithium Cells. *Electrochim. Acta* **2004**, *49*, 979–987. https://doi.org/10.1016/j.electacta.2003.10.009.
(54) Yoshida, K.; Nakamura, M.; Kazue, Y.; Tachikawa, N.; Tsuzuki, S.; Seki, S.; Dokko, K.; Watanabe, M. Oxidative-Stability Enhancement and Charge Transport Mechanism in Glyme-Lithium Salt Equimolar Complexes. *J. Am. Chem. Soc.* **2011**, *133* (33), 13121–13129. https://doi.org/10.1021/ja203983r.
(55) Lee, J.-C.; Litt, M. H. Ring-Opening Polymerization of Ethylene Carbonate and Depolymerization of Poly(Ethylene Oxide-Co-Ethylene Carbonate). *Macromolecules* **2000**, *33*, 11618–11627. https://doi.org/10.1021/MA9914321.
(56) Aurbach, D.; Weissman, I.; Gofer, Y.; Levi, E. Nonaqueous Magnesium Electrochemistry and Its Application in Secondary Batteries. *Chem. Rec.* **2003**, *3* (1), 61–73. https://doi.org/10.1002/tcr.10051.
(57) Chen, X.; Hou, T.; Li, B.; Yan, C.; Zhu, L.; Guan, C. Towards Stable Lithium-Sulfur Batteries : Mechanistic Insights into Electrolyte Decomposition on Lithium Metal Anode. *Energy Storage Mater.* **2017**, *8*, 194–201. https://doi.org/10.1016/j.ensm.2017.01.003.
(58) Pearson, R. G. Hard and Soft Acids and Bases. *J. Am. Chem. Soc.* **1963**, *265* (C). https://doi.org/10.1021/ja00905a001.
(59) Pan, B.; Huang, J.; Sa, N.; Brombosz, S. M.; Vaughey, J. T.; Zhang, L.; Burrell, A. K.; Zhang, Z.; Liao, C. MgCl 2 : The Key Ingredient to Improve Chloride Containing Electrolytes for Rechargeable Magnesium-Ion Batteries. *J. Electrochem. Soc.* **2016**, *163* (8), 1672–1677. https://doi.org/10.1149/2.0821608jes.

(60) Liao, C.; Sa, N.; Key, B.; Burrell, A. K.; Cheng, L.; Curtiss, L. A.; Vaughey, J. T.; Woo, J.-J.; Hu, L.; Pan, B.; et al. The Unexpected Discovery of the $Mg(HMDS)_2/MgCl_2$ Complex as a Magnesium Electrolyte for Rechargeable Magnesium Batteries. *J. Mater. Chem. A Mater. energy Sustain.* **2015**, *3* (11), 6082–6087. https://doi.org/10.1039/c5ta00118h.

(61) Salama, M.; Shterenberg, I.; Shimon, L. J. W.; Keinan-Adamsky, K.; Afri, M.; Gofer, Y.; Aurbach, D. Structural Analysis of Magnesium Chloride Complexes in Dimethoxyethane Solutions in the Context of Mg Batteries Research. *J. Phys. Chem. C* **2017**, *121* (45), 24909–24918. https://doi.org/10.1021/acs.jpcc.7b05452.